

# Greedy Perspectives: Multi-Drone View Planning for Collaborative Coverage in Cluttered Environments

Krishna Suresh<sup>1</sup>, Aditya Rauniyar<sup>2</sup>, Micah Corah<sup>2</sup>, and Sebastian Scherer<sup>2</sup>

**Abstract**—Deployment of teams of aerial robots could enable large-scale filming of dynamic groups of people (actors) in complex environments for novel applications in areas such as team sports and cinematography. Toward this end, methods for submodular maximization via sequential greedy planning can be used for scalable optimization of camera views across teams of robots but face challenges with efficient coordination in cluttered environments. Obstacles can produce occlusions and increase chances of inter-robot collision which can violate requirements for near-optimality guarantees. To coordinate teams of aerial robots in filming groups of people in dense environments, a more general view-planning approach is required. We explore how collision and occlusion impact performance in filming applications through the development of a multi-robot multi-actor view planner with an occlusion-aware objective for filming groups of people and compare with a greedy formation planner. To evaluate performance, we plan in five test environments with complex multiple-actor behaviors. Compared with a formation planner, our sequential planner generates 14% greater view reward over the actors for three scenarios and comparable performance to formation planning on two others. We also observe near identical performance of sequential planning both with and without inter-robot collision constraints. Overall, we demonstrate effective coordination of teams of aerial robots for filming groups that may split, merge, or spread apart and in environments cluttered with obstacles that may cause collisions or occlusions.

## I. INTRODUCTION

The capture of significant events via photos and video has become universal, and Unmanned aerial vehicles (UAVs) extend the capabilities of cameras by allowing for view placement in otherwise hard-to-reach places and tracking intricate trajectories. Multiple aerial cameras can be used to not only view an actor from multiple angles simultaneously but perform higher functions such as localization and tracking [1–3], environment exploration and mapping [3, 4], cinematic filming [5, 6], and outdoor human pose reconstruction [7, 8]. These applications rely on effective collaboration between groups of UAVs whereas manual control may result in poor shot selection and view duplication while requiring many coordinated operators. Therefore, autonomous coordination of UAV teams may be necessary for tasks such as multi-robot filming or reconstruction. However, directly maximizing domain-specific metrics, such as reconstruction accuracy, can be difficult to perform online—this motivates development of proxy objectives that quantify coverage and

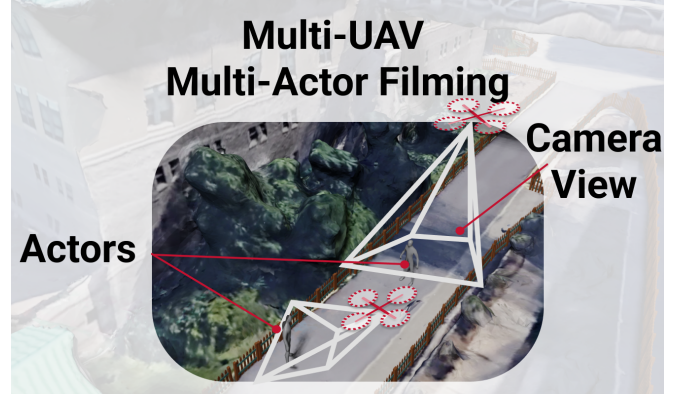


**Fig. 1: Multi-Actor Coverage Scenario:** Known actor and environment geometries as well as actor trajectories and robot start locations are input into the view-planning system. The planner aims to maximize coverage of all actors throughout the planning horizon. Mesh of CMU campus from [9].

detail of multiple views. For example, Bucker et al. [5] demonstrate cinematic filming through a joint objective combining collision and occlusion avoidance, shot diversity, and artistic principles in filming a *single actor*. We are interested in similar settings but where robots collaborate to obtain diverse views of *multiple actors*—in a cluttered environment, with occlusions, and where robots may observe more than one actor at once.

While defining an objective can be difficult, planning for multi-robot aerial systems also presents a significant challenge due to the vast joint state space and non-linear objectives causing optimal planning to be often intractable. Many applications exploit problem-specific structures to reduce the overall search space or alter the search procedure to generate single-robot trajectories sequentially [1–3, 3–5], and Ho et al. [7] describe a single actor-centric drone formation that simplifies the search space. In this work, we apply a planning approach much like Bucker et al. [5] to this multi-actor setting.

**Problem:** The dynamic multi-actor coverage problem consists of generating sequences of camera views over a fixed planning horizon to maximize a collective view reward which is a function of pixel densities over the surfaces of the actors. The primary assumptions required for this problem are: known static environment, known actor trajectories (e.g. scripted scenarios), and known robot start state. An illustration of the problem setup is depicted in Fig. 1. Generating unassigned view plans through the environment allows robots to increase actor coverage and in some cases

<sup>1</sup>K. Suresh is with Olin College of Engineering, Needham, MA, USA ksuresh@olin.edu

<sup>2</sup>A. Rauniyar, M. Corah, and S. Scherer are with the Robotics Institute, School of Computer Science at Carnegie Mellon University, Pittsburgh, PA, USA {rauniyar, micahc, basti}@andrew.cmu.edu

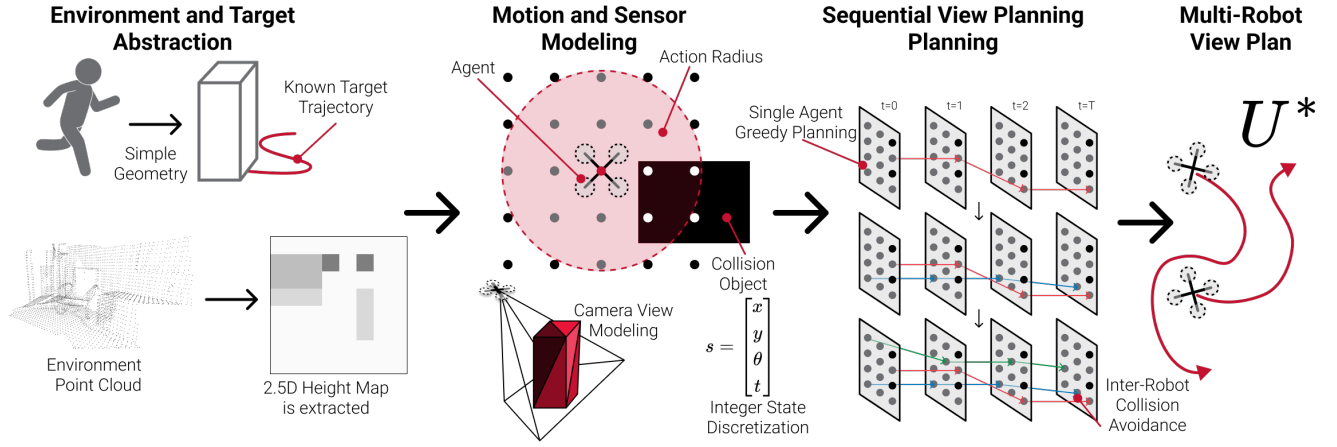


**Fig. 2: Coverage View Planner System Overview** Multi-actor scenario is translated to internal planner representation. Markov Decision Process with DAG encodes collision constraints and coverage objectives. Multi-Robot view plan is produced through sequential greedy planning. Joint multi-drone trajectories are brought back to continuous 3D coordinates and outputted to navigation stack.

require fewer sensors to achieve similar performance.

**Contributions:** The main contributions of this work are summarized as:

- Implementation of a dynamic multi-robot multi-actor view planner.
- Occlusion-aware objective for filming groups of people through software rendering
- Evaluation of such a planner with awareness of inter-robot collisions and comparison against a planner based on fixed formations.

Our contributions build on prior work developing perception objectives based on pixel densities by Jiang and Isler [10] and work by Hughes et al. [11] developing objectives for submodular multi-robot settings. In this work, we present a variant of such objectives that is occlusion-aware, and we present results for scenarios with a wide variety of obstacles and occlusions.

## II. RELATED WORKS

**Aerial Filming:** Aerial perception systems have grown to widespread use through their success in providing low-cost filming of conventionally challenging unscripted scenes. Consumer and commercial systems such as the Skydio S2+ [12] demonstrate single-drone filming capabilities and are starting to incorporate collaborative multi-drone behaviors for mapping. Viable autonomous aerial filming systems for cinematography have been demonstrated by [6] through a multi-drone filming system with a variety of filming and coordination modes.

[7] uses a preconfigured actor-centric formation to optimally view a single actor from multiple angles for human pose reconstruction. This limits the search space to only needing to orient the formation rather than plan each robot individually. [5] allows robots to move through a spherical discretization around a single actor to cinematically film a person. This reduced robot state space allows for rapid

greedy single-robot planning which can be performed sequentially to generate the joint view plan. A key limitation of these approaches is the robot-actor assignment which requires robots to focus observation on a specific actor and may fail to exploit the robots' capacity to observe multiple actors at once. [11] starts to address this challenge by allowing robots to plan over the full environment rather than an actor-centric space, but does not consider inter-robot collisions or environment view occlusions.

**Sequential and Submodular Multi-Robot Planning:** Typically multi-robot perception planning and information gathering problems, cannot tractably be solved optimally due to their combinatorial nature, but greedy methods for submodular optimization can often promise information gain or perception quality no worse than half of optimal in polynomial time [13, 14] Submodular optimization and sequential greedy planning has been applied extensively to such multi-robot coordination problems [1–4, 15–17]. However, questions of occlusions and camera views have been explored primarily in the setting of mapping and exploration [3, 4]. Lauri et al. [16] present an exception in which eye-in-hand cameras inspect and reconstruct static scenes. Unlike exploration and mapping, applications involving filming moving actors can force persistent interaction between robots over the duration of a planning horizon or experiment, and our early work on this topic indicates that sequential planning is important for effective cooperation in this setting [18].

## III. PRELIMINARIES

We will begin with some background regarding submodular and greedy planning:

### A. Submodularity and Monotonicity

Informally, submodularity expresses the principle of diminishing returns and monotonicity requires functions to be always increasing. Given the set of all actions  $\Omega$ , submodularity is defined for a set function  $g$  if  $A \subseteq B \subseteq \Omega$  and  $C \subseteq \Omega \setminus B$ , then  $g(A \cup C) - g(A) \geq g(B \cup C) - g(B)$ . Monotonicity for the same set function  $g$  is defined for any

$A \subseteq B \subseteq \Omega$ ,  $g(A) \leq g(B)$ . This can correspond to our coverage-like objective which diminishes the reward given by duplicate views of the same actor. Objectives related to perception planning [16, 19] and information gathering [15] are often submodular.

### B. Partition matroid

A partition matroid can be used to represent objects product-spaces of actions or trajectories arising in multi-robot planning problems [20, Sec. 39.4]. In the robot planning domain, each robot  $i \in \mathcal{R}$  where  $\mathcal{R} = \{1, \dots, N^r\}$  has access to a set of control actions  $\mathcal{U}_i$ . These actions can take many forms such as assignments, trajectories, or paths. The set of all actions for a robot is the ground set  $\Omega = \bigcup_{i \in \mathcal{R}} \mathcal{U}_i$ . Each robot is assigned one action from its corresponding set  $\mathcal{U}_i$ . If there are no collisions between robots the set of valid and partial control assignments  $\mathcal{S}$  forms a *partition matroid*:  $\mathcal{S} = \{X \subseteq \Omega \mid 1 \geq |X \cap \mathcal{U}_i| \forall i \in \mathcal{R}\}$ . To satisfy this structure each robots' actions must be interchangeable to satisfy the *exchange property* of a matroid. Collisions can violate this property because different actions can conflict with other robots in different ways.

## IV. PROBLEM FORMULATION

We aim to coordinate a team of UAVs to maximize coverage (or observation) of multiple actors through an obstacle-dense environment. Consider a set of actors  $\mathcal{A} = \{1, \dots, N^a\}$  each with a set of faces  $\mathcal{F}_a = \{1, \dots, N^f_a\}$  where  $a \in \mathcal{A}$  and a set of robots  $\mathcal{R} = \{1, \dots, N^r\}$ . Each robot  $i \in \mathcal{R}$  can take action  $u_{i,t} \in U_i \subseteq SE(2)$  at time  $t \in \{0, \dots, T\}$ . Each robot  $i$  will select its plan from its local set of finite-horizon sequences of viable control actions. Additionally, robots have an associated state  $x_{i,t} \in \mathcal{X}$  where  $\mathcal{X}$  is also a subset of  $SE(2)$ .  $\mathcal{X}$  is a shared state space with all robots. Sequences of states a robot's trajectory  $\xi_i = [x_{i,0}, \dots, x_{i,T}]$ , and we will occasionally index trajectories to obtain  $\xi_{i,t} = x_{i,t}$ . Each trajectory, once fixed, produces non-collision constraints for all other robots. Given the trajectories of all actors in  $SE(3)$ , start states  $x_{i,0}$  and environment geometry, we aim to find joint collision-free control sequences  $U^* = \bigcup_{i \in \mathcal{R}} [u_{i,0}, \dots, u_{i,T}]$  that maximize our objective and fit our motion model.

### A. Motion Model

State transitions for each robot are specified by the following motion model:

$$x_{i,t+1} = f_i(x_{i,t}, u_{i,t}) \quad (1)$$

Where  $f_i$  is defined to only allow collision-free actions within the constant velocity constraints. Inter-robot collisions are specified as occurring when robots occupy the same grid cell. Similarly, environment collisions are specified by projecting the environment into the robot's  $SE(2)$  operating plane and ensuring that  $x_{i,t}$  is in free space. Over the time step duration, maximum translational and rotational velocities are converted to bounds on rotation and Euclidean distance as illustrated by Fig. 2.

### B. Sensor Model

We use a coverage-like objective as a proxy for effective observation of an actor. Inspired by [10], observation of faces of each actor  $j$  is captured by the pixel density ( $\frac{px}{m^2}$ ) measured from a linear camera model's image. We can define a function  $\text{pixels}(x_{i,t}, t, j, f) \rightarrow \mathbb{R}$  which returns the pixel density for an actor- $j$ 's face  $f$  when observed from a robot's state at time  $t$ . We then apply a square root to introduce diminishing returns on increasing pixel densities from multiple views [11]. Finally, given robot trajectories according to the dynamics (1) and selected control inputs, the robots obtain the following view reward for the given face and time:

$$R_v(t, j, f) = \sqrt{\sum_{i \in \mathcal{R}} \text{pixels}(x_{i,t}, t, j, f)}. \quad (2)$$

### C. Objective

In addition to maximizing coverage, we add a reward for stationary behavior  $R_s(u_{i,t})$  to reduce unnecessary movement whereas

$$R_s(u) = \begin{cases} \epsilon & \text{if } u \text{ is stationary} \\ 0 & \text{otherwise.} \end{cases} \quad (3)$$

So, robot  $i \in \mathcal{R}$  obtains  $\sum_{t \in \{0, \dots, T\}} R_s(u_{i,t})$  reward for timesteps it remains stationary. The joint objective is then as follows:

$$\mathcal{J}(X_{\text{init}}, U) = \sum_{t \in \{0, \dots, T\}} \left( \sum_{i \in \mathcal{R}} R_s(u_{i,t}) + \sum_{j \in \mathcal{A}} \sum_{f \in \mathcal{F}_j} R_v(t, j, f) \right) \quad (4)$$

where  $X_{\text{init}} = [x_0, \dots, x_{N^r}]$  is an array of initial robot states and  $U$  represents the robots' sequences of control actions. Since we aim to find the control sequence that maximizes this objective, our optimal control sequence can be defined as:

$$U^* = \arg \max_U \mathcal{J}(X_{\text{init}}, U)$$

## V. MULTI-ROBOT MULTI-ACTOR COVERAGE VIEW PLANNER

We now present our multi-UAV coverage view planning system. This planner aims to not only produce sufficient actor coverage but also exploit problem structure to efficiently find single-robot greedy trajectories.

### A. Coverage Representation

To incorporate an occlusion-aware coverage representation we define  $\text{pixels}$  by implementing an OpenGL rasterization renderer which based on a 2.5D height map of our environment and simplified actor geometry. We then use a perspective camera based on our specified camera intrinsics to capture an occlusion-aware representation of what the sensor would expect to see at a given robot state. To render environment occlusions we use a geometry shader to draw the heightmap directly on the GPU. To determine how many pixels we are observing from each face, we render each face

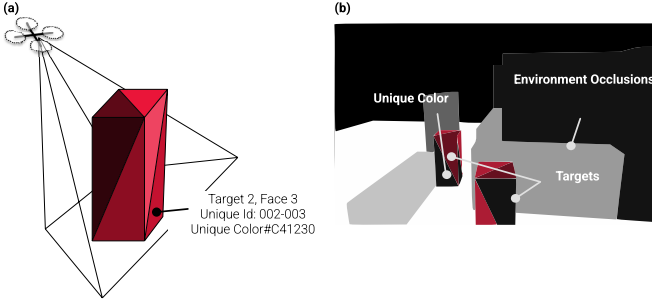


**Fig. 3: Actor Coverage** (a) UAV camera model frustum observing a simplified actor geometry. Actor faces are colored slightly differently based on a face identification system to allow for pixel density computation. (b) Example camera output from OpenGL internal rendering system.

with a unique color that corresponds to an encoding of the actor ID and face ID. We count pixels of each color and divide by the area of the face to obtain the corresponding final pixel density. Figure 3 illustrates this process and provides an example of a rendered view.

### B. Single-Robot Planning

With the robot state in  $SE(2)$  we aim to represent the single-robot planning problem as an MDP which has an underlying DAG structure. The MDP state  $s$  is represented as an integer vector:

$$s = [x \quad y \quad \theta \quad t]$$

Each MDP action  $a$  is in the same discrete space, encoding the next state, and increments the time by 1. This forces the MDP structure to be directed since states can never go back in time. The MDP is constructed with a transition matrix associating  $(s, a, s')$  pair with a transition probability and a reward matrix associating each  $(s, a)$  pair with a reward according to (4) and given other robots' actions (to be introduced next in Section V-C). We perform a breadth-first search over the state space by branch on feasible actions to populate the transition and reward matrices. As depicted in Fig. 2 the set of available actions is pruned based on environment and inter-robot collisions. This directed MDP can be solved with one pass of value iteration to find the optimal greedy policy<sup>1</sup> similarly as by Bucker et al. [5]. Finally, we can follow this policy from our initial state to produce the optimal single-robot control sequence. We use the AI-ToolBox library to represent and solve the MDP [21].

### C. Sequential Planning

Now, we are able to generate the joint view plans for the multi-robot team. We do so by sequentially planning greedy single-robot trajectories as is common for methods based on submodular optimization [2, 5, 15]. This formulation is close to submodular maximization which would yield sub-optimally bounded trajectories, however, our consideration of inter-robot collisions violates the formulation. We explore how the inter collision constraints impact performance in Section VI-D.

<sup>1</sup>Our current implementation converges in 5 passes without exploiting this structure.

### D. Round Robin Planning

Finally, we can extend the sequential planning framework to partially remove the arbitrary prioritization that occurs from the planning order of robots. After the full joint plan is generated, we can iterate through  $\mathcal{R}$ , removing and replanning each robot with all of the previously computed trajectories fixed to improve overall solutions quality much like McCammon et al. [17, Sec. 4.2]. Note that this process can only improve solution quality as the single-robot planner returns optimal solutions and because the current solution is always a valid solution.

---

#### Algorithm 1: Sequential Greedy View Planning

---

```

1 Initialize  $U_{\text{seq}} \leftarrow \{\}$ 
2 Initialize collisionMap  $\leftarrow \{\}$  foreach  $i$  in  $\mathcal{R}$  do
3    $S_i \leftarrow \text{DiscretizeStateSpace}(\text{envHeightMap})$ 
4    $A_i \leftarrow \text{DiscretizeActionSpace}(\text{robotMaxMotion})$ 
5    $\text{MDP} \leftarrow \text{BreadthFirstSearch}(x_{i,0}, S_i, A_i)$ 
   // In BFS,  $R_v$  is computed at each
   // explored state. Branching
   // through availableActions
   // removes actions that lead to
   // collision states.
6    $\pi_i \leftarrow \text{ValueIteration}(\text{MDP})$ 
7    $\{u_{i,0}, \dots, u_{i,T}\} \leftarrow \text{ExtractTrajectory}(\pi_i)$ 
8   Append  $\{u_{i,0}, \dots, u_{i,T}\}$  to  $U_{\text{seq}}$ 
9    $\xi_i \leftarrow \text{applyActions}(x_{i,0}, \{u_{i,0}, \dots, u_{i,T}\})$ 
10  addCollisions( $\xi_i$ )
11 end
12 return  $U_{\text{seq}}$ 

```

---

## VI. EXPERIMENTS

We evaluate the performance of the sequential view planner in five test scenarios that aim to demonstrate view planning under a variety of conditions, and we compare to a formation planning baseline.

### A. Greedy Formation Planning

To compare our coverage planner with an assignment-based view planner, we implement a formation planner modeled off of the multi-view formations described in [7]. We define the formation with a constant radius around an actor and a separation angle  $\phi$ . As described by [7] for  $N^r > 2$  then  $\phi = \frac{2\pi}{N^r}$  and  $\phi = \frac{\pi}{2}$  when  $N^r = 2$  (see Fig. 5). We then select the formation orientation about the actor which maximize the view reward  $R_v$  (including all actors) at each timestep. The formation planner ignores the motion model (Section IV-A) and does not consider environment and robot collisions.

### B. Test Scenarios

Test scenarios, listed in Fig. 6 and Table I, use robots with camera intrinsic parameters of 2500px, 4000px, and 3000px (focal length, image width, image height). All drones are placed at 5 meters high with a camera tilt of 10 degrees



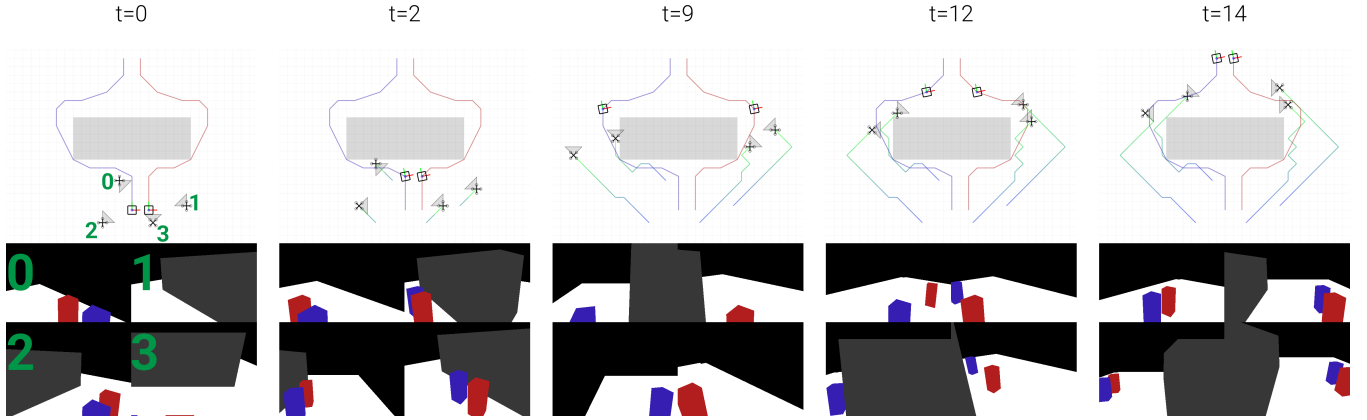


Fig. 4: Example robot views and joint trajectories from sequential plan in *Split* test case. Robot first-person views at each time step display viewing of the actors over the planning horizon.

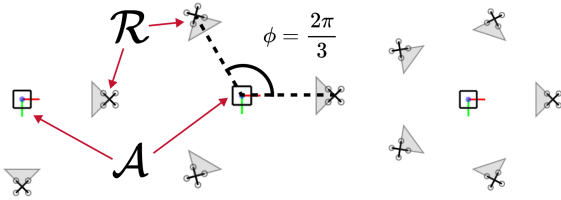


Fig. 5: Multi-robot formations for  $N^r = 2, 3, 5$

Test Name	# Robot	# Actors	Timesteps	Env	Collision
Merge	4	2	17		Yes
Corridor	2	2	17		Yes
Forest	2*	3	20		Yes
Large	18	6	10		No
Split	4	2	15		Yes

TABLE I: Test scenarios and parameters. The formation planner obtains an extra robot in the *Forest* scenario “for free” to match the number of actors

from the horizon. For each test scenario, we also specify 10 unique robot starting configurations to introduce further variation.

*Split*: This test case is a simple group split and merge of 2 actors around an obstacle. A full view sequence from an example trajectory is displayed in Fig. 4.

*Large*: Focuses on scaling to larger teams and features 18 robots. Actors move through a series of short walls that produce occlusions but not collision constraints since they are below the navigation plane.

*Merge*: Contains actors moving around a corner in opposite directions. This test case investigates implicit actor assignment with actors being “handed off” at the corner.

*Corridor*: Tests robots moving through a narrow corridor. This test focuses on the collision-aware aspect of the planner.

*Forest*: This is a dense occlusion/collision environment. This scenario we limit sequential planning to two, fewer than the number of actors (three). This test aims to demonstrate the capacity to adapt to scenarios where assignments are not possible by evaluating if fewer robots can achieve similar

Test	Formation	Seq w/o Inter-Robot	Sequential (ours)
Split	<b>1380</b>	$1352 \pm 34$	$1351 \pm 35$
Large	<b>1413</b>	$1390 \pm 27$	$1381 \pm 27$
Merge	1149	<b>1275 <math>\pm</math> 26</b>	$1274 \pm 28$
Corridor	1612	$1808 \pm 86$	<b>1812 <math>\pm</math> 85</b>
Forest	2114	<b>2534 <math>\pm</math> 73</b>	$2505 \pm 116$

TABLE II: Average and standard deviation of  $R_v$  per robot for all testcases from 10 robot start configurations.

or better coverage compared with the formation planner which requires 3 robots due to the minimum of 1 robot per formation.

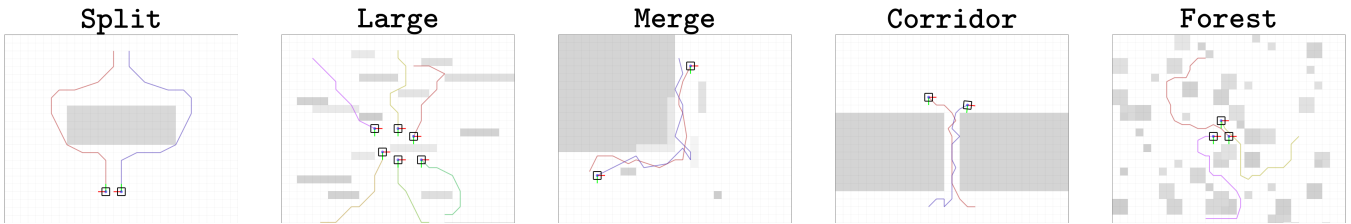
For the purpose of evaluation, we treat both planners as featuring only two robots for the purpose of *per-robot* results.

### C. Sequential Planner Performance

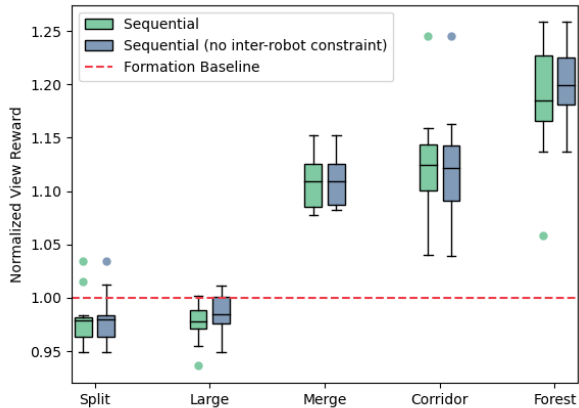
Fig. 7 and Table II summarize planner performance across each of the scenarios in terms of the view reward for formation planning and sequential planning both with and without inter-robot collision constraints. We observe that sequential planning<sup>2</sup> outperforms formation planning in three of five scenarios—by an average of 13.9% in the *Merge*, *Corridor* and *Forest* scenarios. We also observe that inter-robot non-collision constraints do not impair the performance of sequential planning. In the *Split* and *Large* test cases, all planners perform similarly. This may be because these scenarios provide more favorable conditions for the formation planner. *Split* provides ample space for formations of two robots to view the actors, and *Large* has shorter obstacles that produce occlusions but not collisions.

Figure 4 displays the joint view plans and internal view planner renderings for the *Split* test case. This figure illustrates the capacity of sequential planning to optimize views of one or more actors and to implicitly reconfigure or “hand-off” assignments over the course of a trial. The robots all view both actors at  $t = 2$ ; the pairs split off and transition to each viewing a single actor by  $t = 9$ ; and the go back to jointly viewing actors by  $t = 14$ . This behavior

<sup>2</sup>Referring to the collision-free version, but both obtain similar performance.



**Fig. 6:** Scenarios to evaluate specific aspects of multi-actor view planning. Actors are illustrated as boxes with uniquely colored trajectories. The darkness of elements in the height map indicates their occupied height. *Large* is the only test case with no collision obstacles as all elements are below the robot operating plane.



**Fig. 7:** Average view reward normalized by the baseline formation planner performance. 10 unique robot start configurations were specified for the sequential planners and are compared with the unique output from the formation planner. Both sequential planners outperform the formation planner baseline in the *Merge*, *Corridor*, and *Forest* scenarios, or else perform similarly. Both versions of the sequential planner perform similarly in all scenarios; view reward for the collision-aware planner is not impaired, though that planner no longer satisfies guarantees on solution quality.

is not manually specified and arises only from optimizing trajectories and views.

#### D. Inter-Robot Collisions and Round Robin Planning

We also evaluated a 5-iteration round-robot planner (including the initial greedy pass) (Sec. V-D) on the *Merge* scenario. Figure 8 plots view reward as a function of time in the merge for all four planner variants. Here we see similar average performance throughout the duration of the trial for sequential planning with and without inter-robot collision constraints and round-robin planning. In this scenario, incrementally improving the solution via round-robin planning does not significantly improve solution quality. Near the middle of the trajectory, we see similar view performance among all planners corresponding to the incidental viewing of both actors by the formation planner and the intended collaborative viewing from the sequential planners.

### VII. CONCLUSION AND FUTURE WORK

In this work, we present a novel system for multi-robot view planning through sequential greedy planning with an occlusion-aware objective. Through preliminary evaluation in

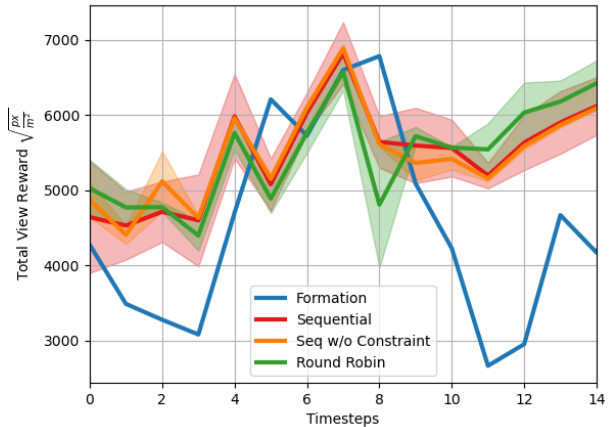


**Fig. 8:** Total view reward over time for *Merge* test case averaged across 10 trials. Incremental updates to the solution via round-robin planning do not significantly improve solution quality in this scenario. The planning approaches we propose (sequential planners and round-robin) provide more consistent view reward over the duration of the trial compared to the formation planner which exhibits dips in performance at either end of the trial.

five scenarios, we observe sequential planning outperforming formation-based planning and specifically excelling in occlusion-dense environments. Additionally, we find similar performance for sequential planning with and without inter-robot collision constraints demonstrating that sequential planning performs well even without bounded suboptimality. Finally, we show preliminary results of round-robin planning achieving greater stability in view reward through the joint trajectory. In future work, we aim to extend the view planning system to consider sequence order, deploy view plans to a 3D human pose reconstruction task, and optimize our implementation to run at real-time rates.

#### ACKNOWLEDGMENT

This work is supported by the National Science Foundation (NSF) under Grant No. 2024173. Krishna was sponsored by the NSF REU program, as a part of the Robotics Institute Summer Scholars (RISS) program.

#### REFERENCES

- [1] M. Corah and N. Michael, “Scalable distributed planning for multi-robot, multi-target tracking,” in *Proc. of*

- the *IEEE/RSJ Intl. Conf. on Intell. Robots and Syst.*, Prague, Czech Republic, Sep. 2021.
- [2] X. Cai, B. Schlotfeldt, K. Khosoussi, N. Atanasov, G. J. Pappas, and J. P. How, “Energy-aware, collision-free information gathering for heterogeneous robot teams,” *IEEE Trans. Robotics*, vol. 39, pp. 2585–2602, 2023.
  - [3] B. Schlotfeldt, V. Tzoumas, and G. J. Pappas, “Resilient active information acquisition with teams of robots,” *IEEE Trans. Robotics*, vol. 38, no. 1, pp. 244–261, 2021.
  - [4] M. Corah and N. Michael, “Distributed matroid-constrained submodular maximization for multi-robot exploration: theory and practice,” *Auton. Robots*, vol. 43, no. 2, pp. 485–501, 2019.
  - [5] A. Buckner, R. Bonatti, and S. Scherer, “Do you see what I see? Coordinating multiple aerial cameras for robot cinematography,” in *Proc. of the IEEE Intl. Conf. on Robot. and Autom.*, Xi’an, China, May 2021.
  - [6] A. Alcántara, J. Capitán, A. Torres-González, R. Cunha, and A. Ollero, “Autonomous execution of cinematographic shots with multiple drones,” *IEEE Access*, vol. 8, pp. 201 300–201 316, 2020.
  - [7] C. Ho, A. Jong, H. Freeman, R. Rao, R. Bonatti, and S. Scherer, “3D human reconstruction in the wild with collaborative aerial cameras,” in *Proc. of the IEEE/RSJ Intl. Conf. on Intell. Robots and Syst.*, Sep. 2021.
  - [8] N. Saini, E. Price, R. Tallamraju, R. Enfiacud, R. Ludwig, I. Martinovic, A. Ahmad, and M. J. Black, “Markerless outdoor human motion capture using multiple autonomous micro aerial vehicles,” Seoul, South Korea, 2019, pp. 823–832.
  - [9] C. Cao, H. Zhu, F. Yang, Y. Xia, H. Choset, J. Oh, and J. Zhang, “Autonomous exploration development environment and the planning algorithms,” in *2022 International Conference on Robotics and Automation (ICRA)*, 2022, pp. 8921–8928.
  - [10] Q. Jiang and V. Isler, “Onboard view planning of a flying camera for high fidelity 3D reconstruction of a moving actor,” Jul. 2023. [Online]. Available: <http://arxiv.org/abs/2308.00134>
  - [11] S. Hughes, M. Corah, and S. Scherer, “Towards informed multi-robot planners for group reconstruction,” *Robotics Institute Summer Scholar’ Working Papers Journals*, 2022, in preparation for submission to ACC 2024.
  - [12] “Drone That Follows You - Skydio 2+ | Skydio.” [Online]. Available: <https://www.skydio.com/skydio-2-plus/>
  - [13] G. L. Nemhauser, L. A. Wolsey, and M. L. Fisher, “An analysis of approximations for maximizing submodular set functions-I,” *Math. Program.*, vol. 14, no. 1, pp. 265–294, 1978.
  - [14] M. L. Fisher, G. L. Nemhauser, and L. A. Wolsey, “An analysis of approximations for maximizing submodular set functions-II,” *Polyhedral Combinatorics*, vol. 8, pp. 73–87, 1978.
  - [15] A. Singh, A. Krause, C. Guestrin, and W. J. Kaiser, “Efficient informative sensing using multiple robots,” *J. Artif. Intell. Res.*, vol. 34, pp. 707–755, 2009.
  - [16] M. Lauri, J. Pajarinen, J. Peters, and S. Frintrop, “Multi-sensor next-best-view planning as matroid-constrained submodular maximization,” *IEEE Robot. Autom. Letters*, vol. 5, no. 4, pp. 5323–5330, 2020.
  - [17] S. McCammon, G. Marcon dos Santos, M. Frantz, T. P. Welch, G. Best, R. K. Shearman, J. D. Nash, J. A. Barth, J. A. Adams, and G. A. Hollinger, “Ocean front detection and tracking using a team of heterogeneous marine vehicles,” *J. Field Robot.*, vol. 38, no. 6, pp. 854–881, 2021.
  - [18] M. Corah, “On performance impacts of coordination via submodular maximization for multi-robot perception planning and the dynamics of target coverage and cinematography,” in *RSS 2022 Workshop on Envisioning an Infrastructure for Multi-Robot and Collaborative Autonomy Testing and Evaluation*, 2022.
  - [19] M. Corah and N. Michael, “Volumetric objectives for multi-robot exploration of three-dimensional environments,” in *Proc. of the IEEE Intl. Conf. on Robot. and Autom.*, Xi’an, China, May 2021.
  - [20] A. Schrijver, *Combinatorial optimization: polyhedra and efficiency*. Springer Science & Business Media, 2003, vol. 24.
  - [21] E. Bargiacchi, D. M. Roijers, and A. Nowé, “AI-Toolbox: A C++ library for reinforcement learning and planning (with Python bindings),” *Journal of Machine Learning Research*, vol. 21, no. 102, pp. 1–12, 2020.